Supporting Information

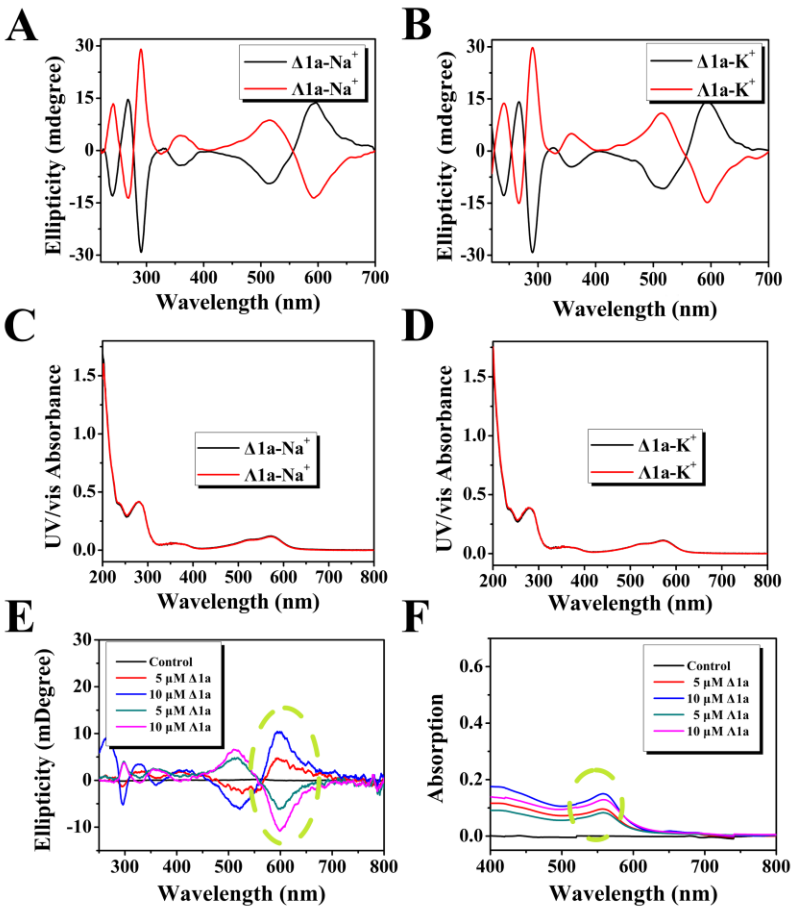

Figure S1. CD spectra of **Δ1a** (black) and **Λ1a** (red) measured in Na^+ buffer (A) and K^+ buffer (B). The CD spectra were measured at the concentration of 10 μM for each enantiomer in 10 mM Tris buffer (pH 7.2) containing 10mM KCl or 100mM NaCl. The UV-vis profiles of **Λ1a** (red) and **Δ1a** (black) acquired from Na^+ buffer (C) and K^+ buffer. (D) in 10 mM Tris-HCl buffer (pH = 7.2). (E) The CD spectra of the cell culture media with different amounts of metal complexes. Control is the cell culture media. (F) The absorption spectra of the cleared lysate with different amounts of metal complex. Control is the cleared lysate.

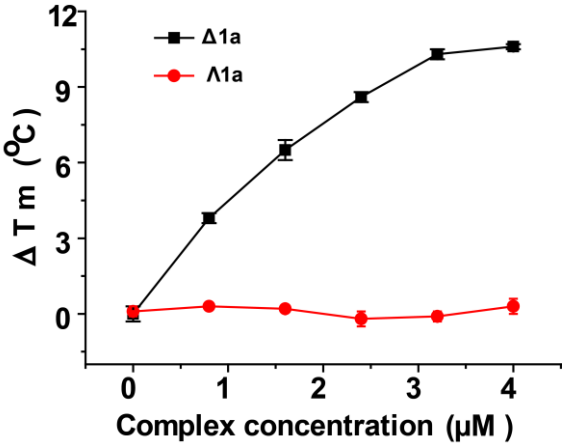

Figure S2. Variations of the melting temperature ΔT_m for Tel22 binding to **Λ1a** and **Δ1a** were plotted versus the concentration of complexes. Tel22 concentration was 4 μM in strand. The assays were carried in 10 mM Tris buffer (pH 7.2) containing 10 mM KCl.

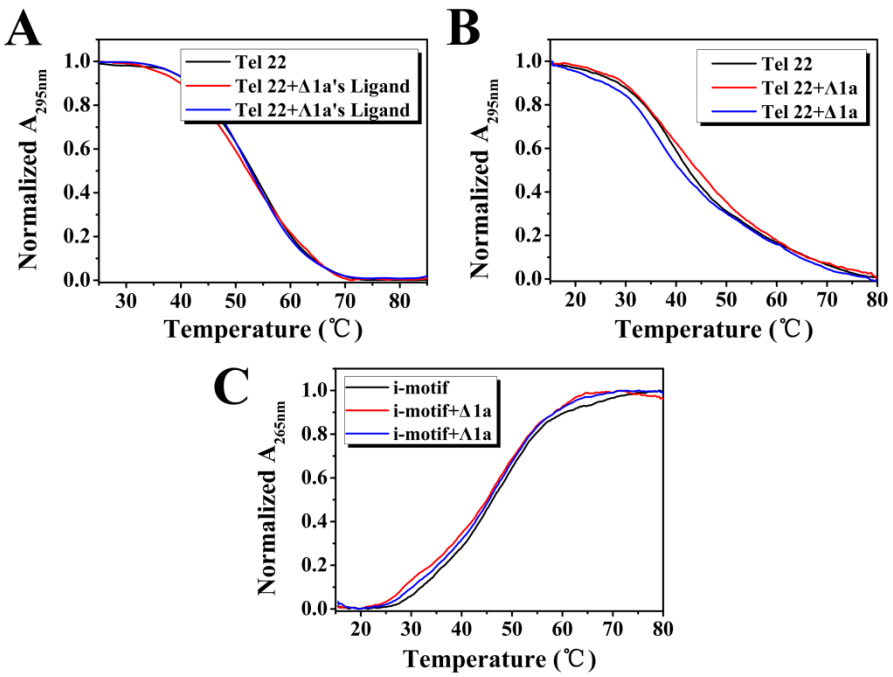

Figure S3. (A) The UV melting profiles of the Tel22 in the absence and presence of equivalent enantiomers' ligand in 10 mM KCl, 10 mM Tris buffer (pH 7.2). (B) The UV melting profiles of Tel22 in the absence and presence of equivalent enantiomer in 10 mM NaCl, 10 mM Tris buffer (pH 7.2). (C) The UV melting profiles of i-motif in the absence and presence of equivalent enantiomer in 10 mM KCl, 10 mM Tris buffer (pH 5.5).

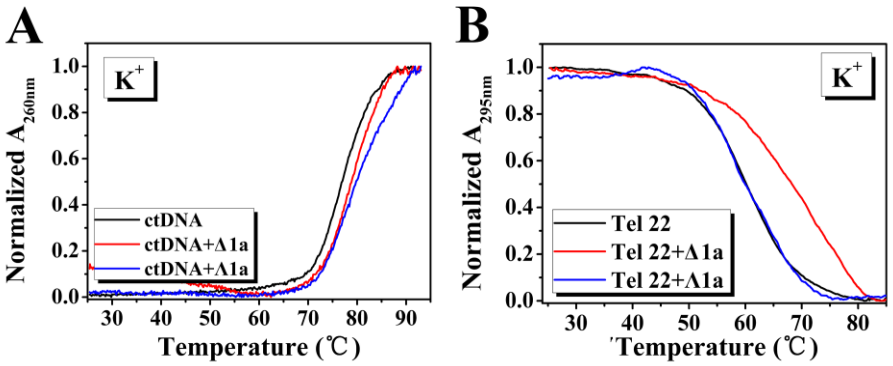

Figure S4. (A) UV melting profiles of ctDNA in the absence and presence of **Δ1a/Λ1a** in 30 mM KCl, 10 mM Tris buffer (pH 7.2). (B) UV melting profiles of Tel22 in the absence and presence of **Δ1a/Λ1a** in 30 mM KCl, 10 mM Tris buffer (pH 7.2).

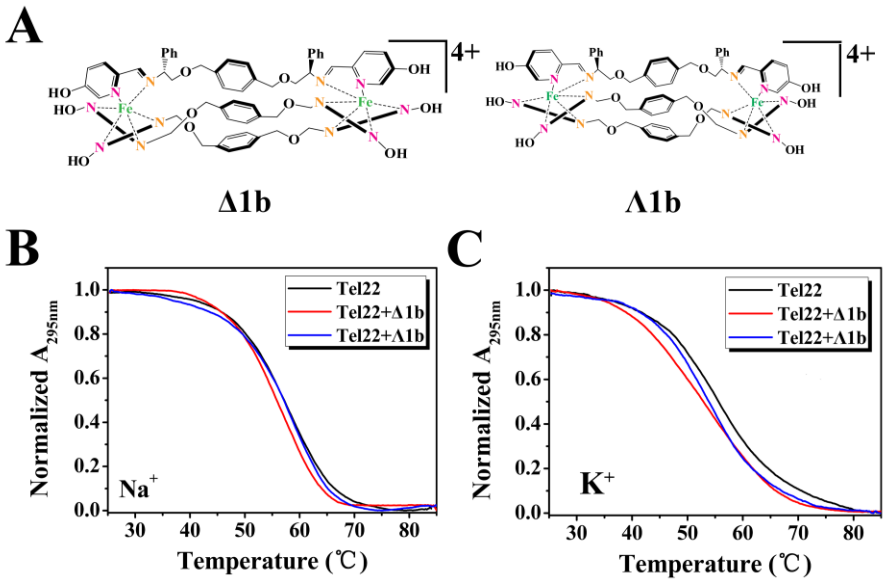

Figure S5. (A) Structure of **Δ1b** and **Λ1b** cation. UV melting profiles of the Tel22 in the absence and presence of **Δ1b** or **Λ1b** obtained from Na^+ buffer (B) and K^+ buffer (C). The UV melting profiles were measured in 10 mM Tris buffer (pH 7.2) containing 10mM KCl or 100mM NaCl. The concentration of the enantiomers was equivalent with the strand concentration of Tel22.

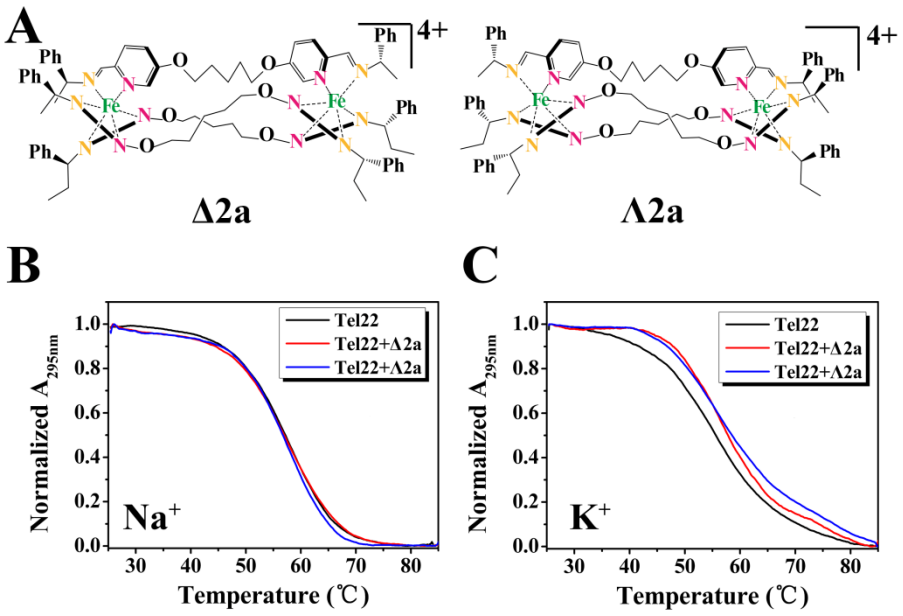

Figure S6. (A) Structure of **Δ2a** and **Λ2a** cation. UV melting profiles of the Tel22 in the absence and presence of **Δ2a** or **Δ2a** obtained from Na^+ buffer (B) and K^+ buffer (C). The UV melting profiles were measured in 10 mM Tris buffer (pH 7.2) containing 10mM KCl or 100mM NaCl. The concentration of the enantiomers was equivalent with the strand concentration of Tel22.

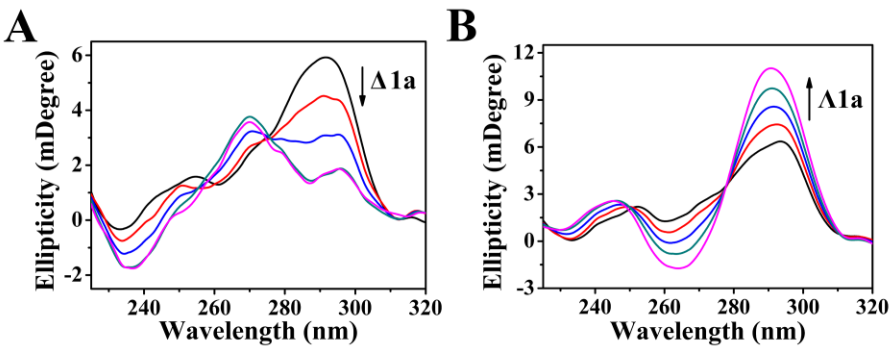

Figure S7. CD titration of Tel22 with **Δ1a** (A) and **Λ1a** (B) in 10 mM KCl, 10 mM Tris buffer (pH 7.2). The concentration of the enantiomer was varied from 0 μM to 2 μM.

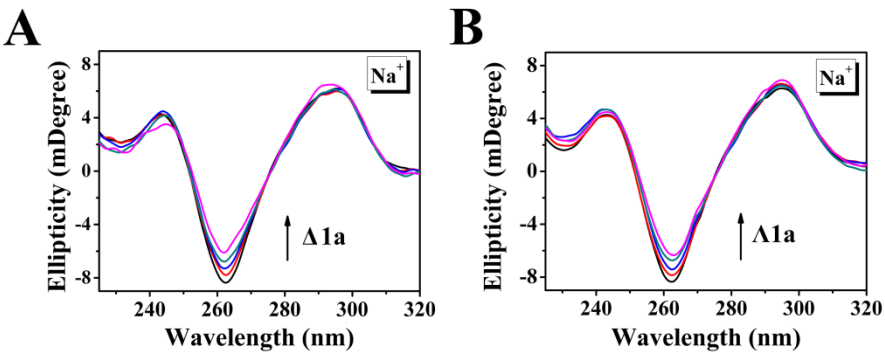

Figure S8. CD titration of Tel22 with **Δ1a** (A) and **Λ1a** (B) in 100 mM NaCl, 10 mM Tris buffer (pH 7.2). The concentration of enantiomer was varied from 0 μM to 4 μM.

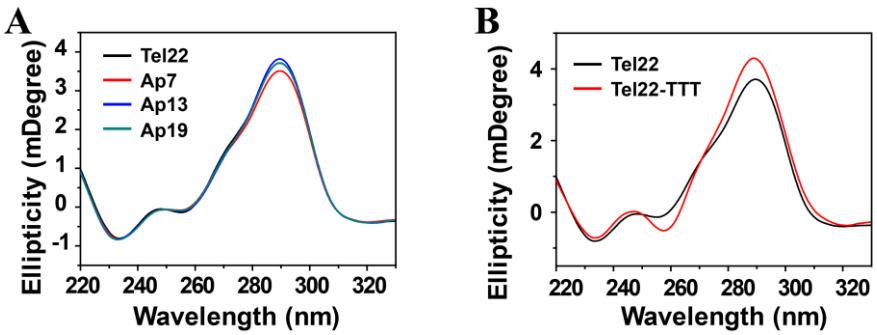

Figure S9. (A) CD spectra of Tel22, Ap7, Ap13 and Ap19. (B) CD spectra of Tel22 and Tel22-TTT. The assays were carried out in 100 mM KCl, 10 mM Tris buffer (pH 7.2).

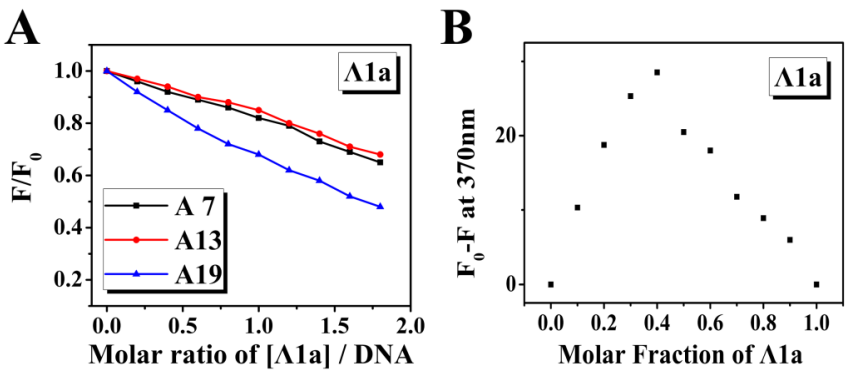

Figure S10. (A) Plot of normalized fluorescence intensity at 370 nm of 2-Ap individually labeled Tel22 versus molar ratio of **Λ1a** /DNA in 10 mM KCl, 10 mM Tris buffer (pH 7.2). The concentration of the 2-Ap labeled Tel22 was 0.5 μM. (B) Job's plot for complexation of **Λ1a** and Ap19-Tel22. [**Λ1a**]+[Ap19-Tel22]=0.3 μM.

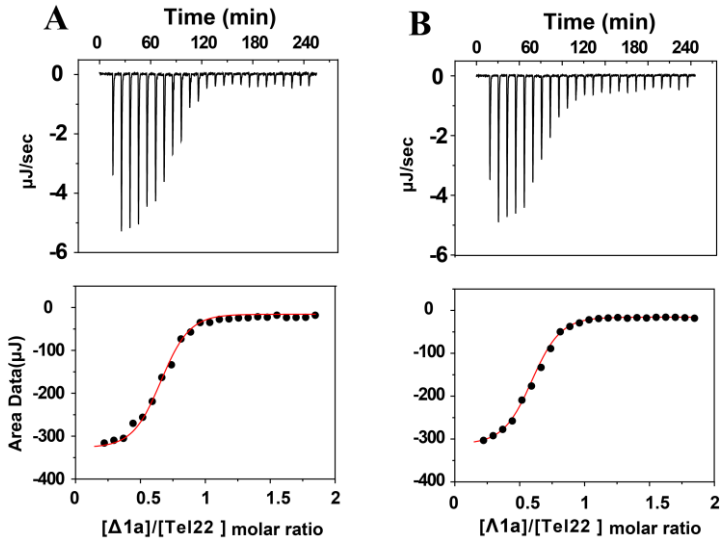

Figure S11. Representative ITC data for the binding of Tel22 with **Δ1a** (A) and **Λ1a** (B). Titrations were performed in 10 mM Tris-HCl buffer, 10 mM KCl, pH = 7.2.

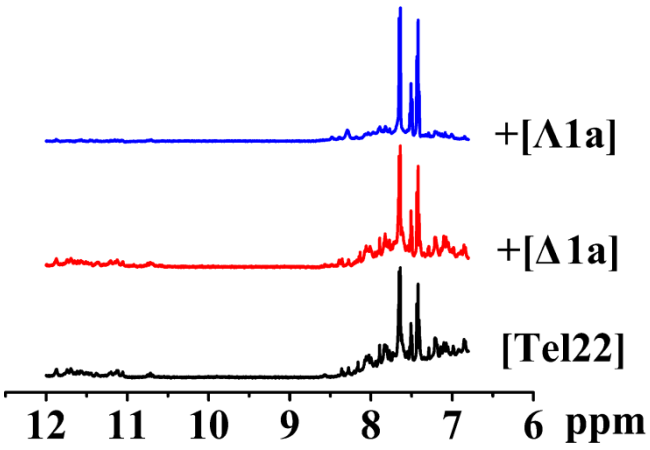

Figure S12. NMR titration of Tel22 with **Δ1a** and **Λ1a**.

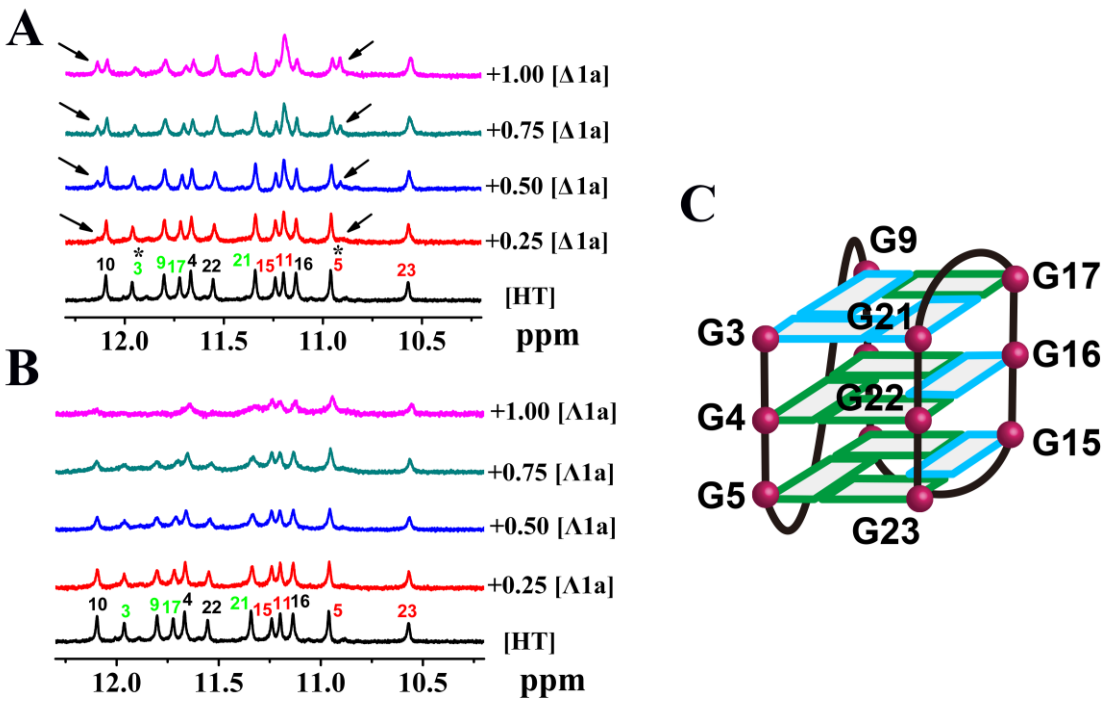

Figure S13. ^{1}H NMR titration of HT with **Δ1a** (A) and **Λ1a** (B) at various [Ligand]/[HT] ratios. The profiles were measured in 10 mM Tris-10 mM KCl buffer containing 10% D_2O. Peaks of G3 and G5 are labeled with stars. (C) The structure of hybrid-1 G-quadruplex formed by HT. Anti and syn guanines are colored green and blue, respectively. HT is the DNA sequence that can form homogeneous hybrid-1 G-quadruplex in K^+ (1, 2).

.

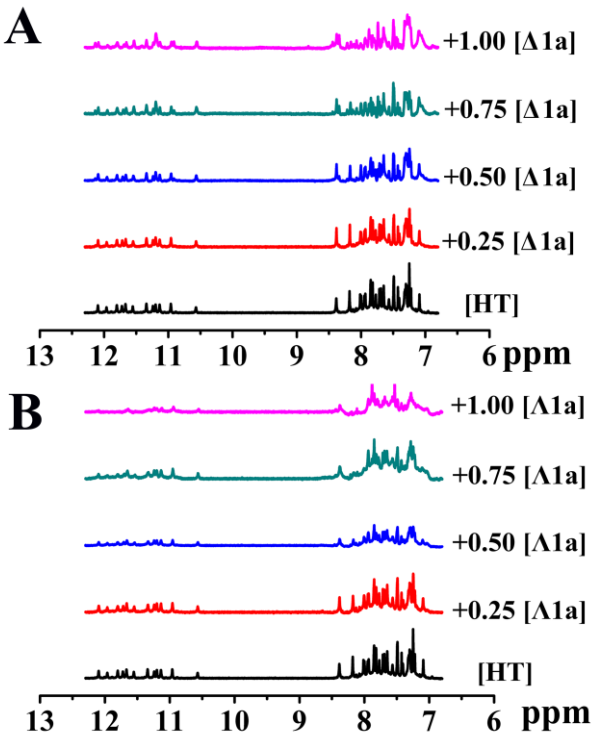

Figure S14. NMR titration of HT with **Δ1a** and **Λ1a**.

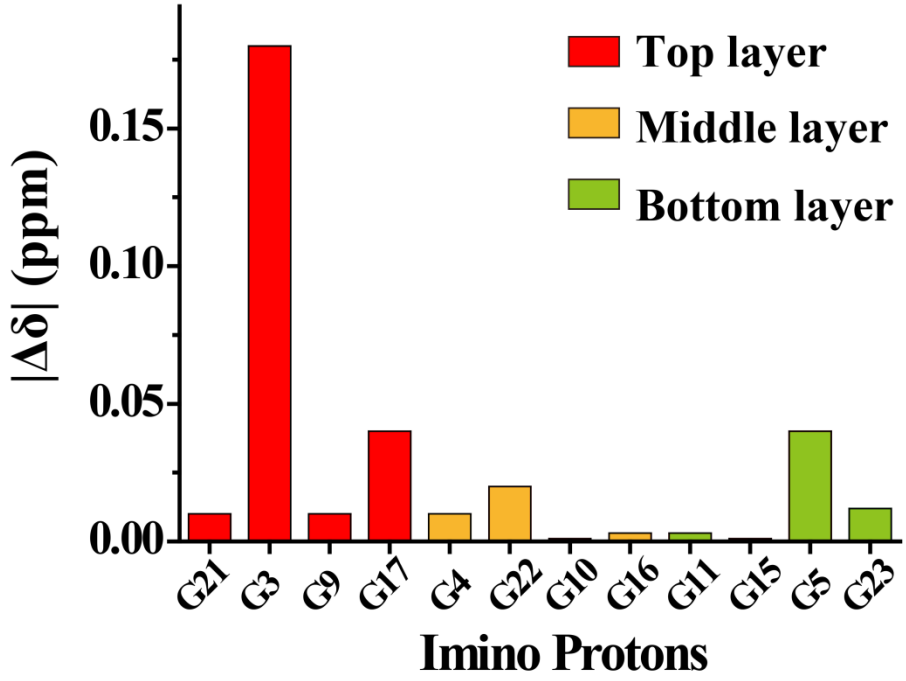

Figure S15. Diagram showing the change in the chemical shift of each imino (H1) proton (**Δ1a**).

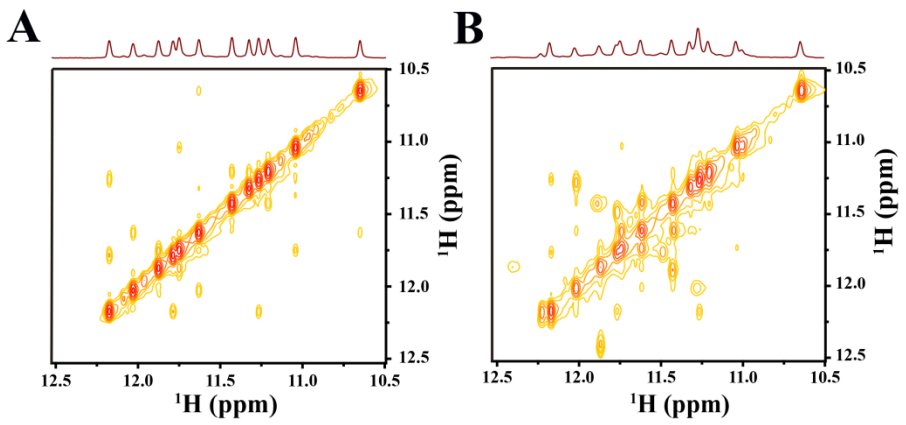

Figure 16. NOESY spectrum (mixing time, 200 ms) of HT (A) and HT in the presence of 50% **Δ1a** (B). HT was prepared in water containing 20 mM KCl and 10% D_2O.

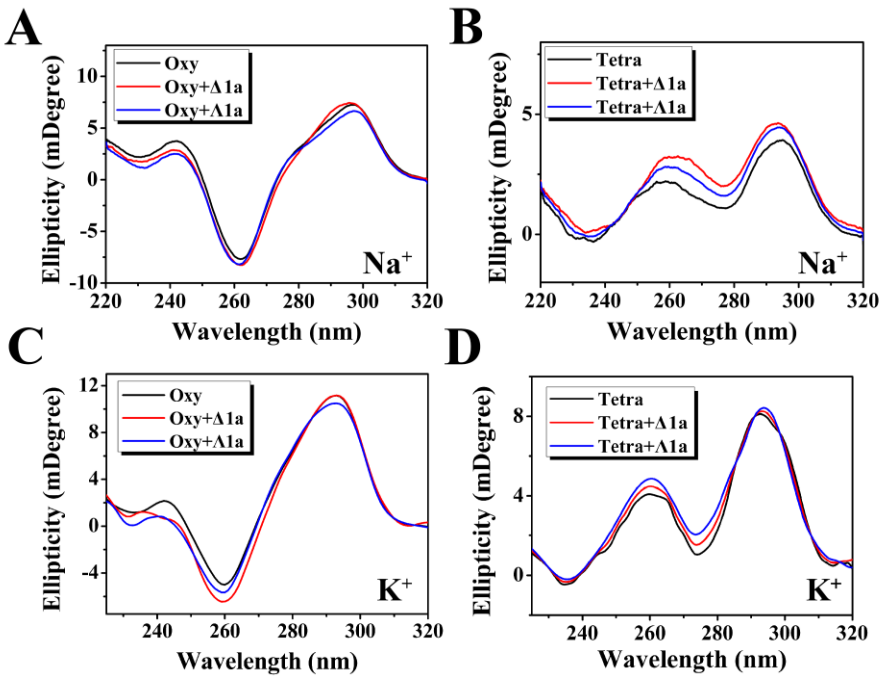

Figure S17. CD spectra of different G-quadruplex DNAs in the absence and presence of enantiomers in Na^+/K^+ containing buffer.

Table S1. Stabilization effect of **Δ1a** and **Λ1a** on different telomeric G-quadruplex DNA in Na^+ containing buffer. [a]

Telomeric DNA	Structure	DNA T_m (℃)	+Δ1a ΔT_m (℃)	+Λ1a ΔT_m (℃)
Human (Tel22)	Antiparallel	59.0 ±0.3	0.1 ±0.2	0.2 ±0.3
Oxytricha	Antiparallel	62.9 ±0.2	-2.7 ±0.2	-3.5 ±0.4
Tetrahymena	Hybrid	62.1 ±0.2	-1.4 ±0.4	-1.5 ±0.2

[a]Melting assays were carried out in 10 mM Tris buffer containing 100 mM NaCl at pH 7.2. DNA is 3 μM in strand. The concentration of the Ligands is equivalent with corresponding DNA. The values were the average of three independent measurements.

References:

1. Luu, K.N., Phan, A.T., Kuryavyi, V., Lacroix, L. and Patel, D.J. (2006) Structure of the Human Telomere in K+ Solution: An Intramolecular (3 + 1) G-Quadruplex Scaffold. *J. Am. Chem. Soc.*, **128**, 9963-9970.
2. Chung, W.J., Heddi, B., Tera, M., Iida, K., Nagasawa, K. and Phan, A.T. (2013) Solution Structure of an Intramolecular (3 + 1) Human Telomeric G-Quadruplex Bound to a Telomestatin Derivative. *J. Am. Chem. Soc.*, **135**, 13495-13501.
3. Jaumot, J. and Gargallo, R. (2012) Experimental methods for studying the interactions between G-quadruplex structures and ligands. *Curr. Pharm. Des.*, **18**, 1900-1916.